Understanding the Importance of Double Coated Paper Structure in Printing

Patrice J. Mangin[1], Claude Daneault[1], Martin Dubé[1], and Daniel Matte[2]

Keywords: Coated paper, structure studies, printability, ink flow

Abstract

Double coated papers are usually high quality paper grades. The double coating structure contains a precoat, which usually serves to fill-in the surface pores while the topcoat, which will be printed on, is of a higher quality. We have investigated the effect of the precoat on the printing characteristics of double coated papers as measured by the Deltack method. We found that both the precoat and the topcoat influence the final ink holdout. We propose a model based on preferential filtration and pigment packing that varies from the precoat to the topcoat to explain how the precoat may be used to improve the printing characteristics of papers.

The model is based on preferential filtration of ink components on the topcoat structure while the topcoat structure is itself controlled by the precoat. As a consequence, it is possible to obtain the same maximum in the Deltack force (which is an evaluation of ink holdout and force exerted on the paper surface) with very different double coated paper structures having either the same pore diameters and different pore volumes or having the same pore volume but different pore diameters. The pore volume and pore diameters can be modified and optimized by changing the mineral pigments included in the coating colour.

1. Introduction

The need to improve paper properties is always what consumers request from the printers and the paper producers. As coated paper is a big part of the improvement, there is a need for high performance coatings. Coatings are applied to board and paper to provide a smooth surface and to improve the printing snap, often defined as the overall impression of the print quality as perceived through human eyes in

1 University of Quebec in Trois-Rivieres, Canada; 2 International Coating Centre (CIC), Trois-Rivières, Canada.

the pressroom. Most studies are performed to identify the best pigment-binder combinations and thus obtain the right properties required by the papermaker for operations. The type and the amount of the various coating colour components affect the mechanical, optical and liquid absorption characteristics of the coated paper in a very complex manner. This is particularly true for the offset printing process where a large amount of ink and water, up to 300% ink coverage through 4, and more, ink layer applications, are added to the paper during printing. A properly formulated coating offers several options and the papermaker is continuously looking for new ways to take advantage of formulation options to improve properties such as brightness, opacity, smoothness, surface strength, ink setting, ink drying, print gloss, etc. (Karathanasis *et al*, 2001).

In the last 2 decades, several studies tried to explain the factors that control the printability of the coated paper. The pore structure of paper coatings that could be modified using a range of different mineral pigments and binder contents, has been found by many researchers to have a significant effect on the coated paper printing characteristics (Preston *et al*, 2001). The first identified paper structure parameter was the architecture of the pore structure for the base paper and the coating layer which together drive the final print properties. Most physical and functional properties of pigment coated papers are influenced to a greater or lesser extent, by the porous structure of the coating layer. For example, the number and the size of microvoids contribute to macroscopic properties such as brightness, light scattering efficiency, and opacity. The void structure also affects the flow of liquids and gases through the coating layer. Absorption of inks and fountain solutions during printing is controlled by the structure of the pore space close to the coating layer surface. The porous structure of a coating layer depends on the coating colour formulation, pigments and their combinations, synthetic and natural binders, chemical additives (e.g. associative thickeners), coating colour application, and the drying processes (Toivakka and Nyfors, 2000). Therefore, it becomes obvious that the coated paper structure can be considered as a combination of fibres, pigment(s), binder, and air volume. The literature is then closely related to the pore structure or network: a concept with its own terminology.

The application of a coating layer is a complex process dependent of many interactions between the components and the process. Notwithstanding various factors, the application must still be achieved on a paper surface designed to adequately receive a layer of coating. As the coating layer does not and will not hide a defect or enhance the poor quality of the base paper, base paper characteristics are very important to obtain a high quality final product and insure good printability (Drage *et al*, 1999; Zou *et al*, 2002). The coating layer applied on the base stock or another coating layer is mainly produced with minerals pigments and latex. Coating structure design may be achieved by modeling the pigment particle size and particle size distribution. The pigment particle size determines the paper gloss, while the pore size is determined by both the particle size and the distribution.

While the pigments create the structure, the latex keeps the structure holding together after drying in the coating process. Latex has a complex chemical structure. It is composed of particles and liquid forming an emulsion. The type and particle size of the latex give the final properties of the film formed when the sheet is dried. The latex is one of main components used to increase the strength of the coating structure. The type and particle size of the latex also affect the coating structure.

Double layer coating is used to obtain a paper with maximum gloss and printability characteristics (Eng, 2002). Usually, double-coating is used to apply high coat weight applications as it mainly provides a large flexibility for the coating colours and coat weights, in both the precoat and the topcoat layer, applied on the paper. It should be emphasized that with the same total coatweight, double-coating provides a paper with a smoother surface after printing than single-coating where fibre swelling will increase the paper surface roughness (Grön and Rautiainen, 1999, Renvall *et al*, 1990). The interactions between the coating layers and the base paper are critical parameters to consider when producing a new or a modified coated paper grade. Multilayer coating is generally done to apply high coat weights in a strategy to minimize total production cost.

Some studies indicate that both a) the coatweight of the precoat and the method of precoat application have also a predominant influence on the final product (Renvall *et al*, 1990), and b) the coatweight/coating colour interaction between each layer and the base paper directly also controls the final quality of the paper (Renvall *et al*, 1990, Hassell *et al*, 1989). It should also be noted that the identification of an exact "layer" and of the separation lines between layers in a double coated paper is not clearly defined. Indeed, as seen in Figure 1a, one could follow a probable line that would separate the paper base stock from the precoat layer, and another probable line that would separate the precoat from the topcoat layer. In reality, the separation zones are not as clearly defined and some interaction and interpenetration between the layers is to be expected (Figure 1b).

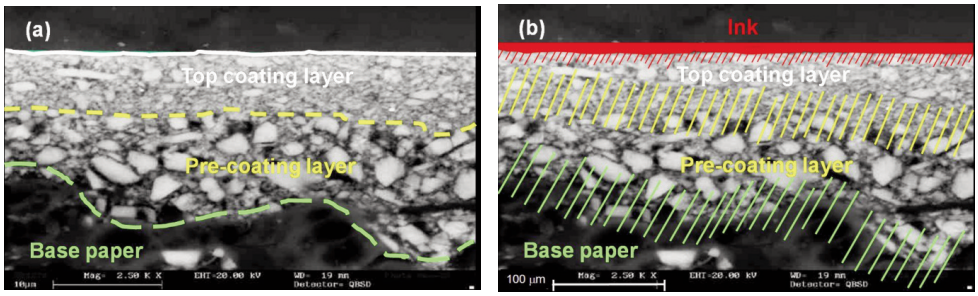

Figure 1 *– Double coated paper structure showing (a) separation line between base paper, precoat and topcoat layers, and (b) most probable interaction zones (instead of true separation lines).*

From the literature review, it is apparent that the double coated papers properties in relationship with above concepts have not been largely and fundamentally analysed. It is especially true when considering the architecture of the pore structure in the various layers in relationship to the double-coated paper properties: little understanding of the true fundaments exits. Most of the studies evaluate the effect of the precoat on the final printability but are limited to the single precoated paper: under-standing of the interaction between the two layers and on the final topcoat is still somehow lacking. Our research objective was then to study the characterization of the different layers in order to understand and propose the mechanisms and interactions of how the layer truly affects the final coated paper property as we surmised such an understanding to be a key factor to improving the printing characteristics and quality of double-coated papers.

2. Method of Evaluation

2.1 Materials and Processes

We learned from the literature study that the precoat has a significant influence on the top coat properties but that the effect of the different components and parameters of the precoat are yet to be established. Accordingly, we designed the experimental study to analyse the effect of key precoat parameters on the topcoat properties. From standard precoat composition (initial conditions or Group 0), i.e. a precoat containing 100 parts ground calcium carbonate (GCC) which is the case of about 98% of commercial precoat, we modified the precoat components/parameters by:

1. replacing 20% of the GCC by clay (later called 20% clay substitution): group samples 1 or Group 1,

2. calendering either the base paper or the precoat before precoat and/or top coat application: Group 2,

3. substituting the standard precoat latex by an acrylic latex and the carboxy methyl cellulose (CMC) by an amphoteric thickener i.e. protein: Group 3,

4. replacing 100% of the standard GCC by different GCC or precipitated calcium carbonates (PCC) or Brazilian clay: Group 4.

The experimental design is schematically represented in Table 1.

In practice, above conditions corresponds to a total of 20 “precoat conditions”: 1 for the initial condition (Group 0), 4 for the 20% clay substitution (Group 1), 4 for the calendering of the base paper, the precoat being uncalendered (Group 2A) and 4 when the precoat is calendered but not the base paper (Group 2B), 2 for the latex/CMC substitution (Group 3), and 4 for the 100% pigment substitution (Group 4).

On top of all these 20 precoat conditions we applied 3 different topcoats for a total of 60 conditions (3 x 20). All 60 samples were calendered to a gloss target of 70 (Allem and Uesaka, 1999).

For the 3 topcoats we used 3 different latexes with the same pigments and additives systems. The 3 latexes used are styrene /butadiene /acrylonitrile latex (S/B/ACN), styrene/acrylic latex (S/A), and styrene/acrylic/acrylonitrile latex (S/A/ACN).

It should be emphasized that only Group 1 (20% clay substitution) and Group 4 (100% clay substitution) are presented here.

The technical characteristics of the 3 latexes used for the topcoats and for the precoats are listed in Appendix (Table A1).

PRECOATED FORMULATION	GROUP	SPECIFIC OBJECTIVE
100 parts GCC (1.4 μm)	Control	Reference (as used by industry standards)
		STUDYING THE EFFECT OF
GROUP 1	20 parts pigment substitution	Replacing 20 parts GCC by various kaolin clays
GROUP 2	Pre-calendering base paper/precoat	Pre-calendering on structure and printing characteristics
GROUP 3	Latex and protein	Latex modification and/or thickener on structure
GROUP 4	100 parts pigment substitution	Replacing GCC with other pigments

Table 1 *– Experimental Design (Schematic)*

The precoat applications were performed in a roll form on a pilot coater at CIC pilot coater facility (*An., Centre International du Couchage*) using the jet applicator coating head. The precoat formulations for the 20 (Table A2) and 100% (Table A3) clay substitutions are presented in Appendix. The calendaring of the base paper and the precoat were done by soft nip calendering on the CIC pilot coater. The topcoat applications on the 20 precoated rolls were done on a CLC 7000 (Cylindrical Laboratory Coater or CLC) at CIPP. The final 60 topcoated samples were calendered on a laboratory supercalender at CIC. The complete formulations, calendaring conditions, and coater settings are listed in Appendix. Although twelve different rolls from the same base stock were used to make the 20 precoated conditions, the results indicated that the base stock paper is very consistent and stable. All the precoated rolls were coated both sides on the pilot coater (as a control for curl). The rougher side was coated first. The precoat operations conditions of the pilot coated are presented in Appendix (Table A4).

The formulations used for the top coat (CLC 7000) are listed in Appendix (Table A5). The CLC conditions for the coating are as follows: speed of 800 m/min, pre-heating

of 10 seconds at 80% intensity, drying time of 30 seconds at 100% intensity, and coating length of 5 meters (on a 760 mm width). The coating blade is 0.457 mm thick with a 50° tip angle.

As the precoat was applied on both sides of the base stock paper, the top coating was always applied on the same precoat side: the one corresponding to the smooth side of the base paper as seen in Figure 2 below.

When adding the top coat layer, each CLC coating run provides a 14 cm wide coated

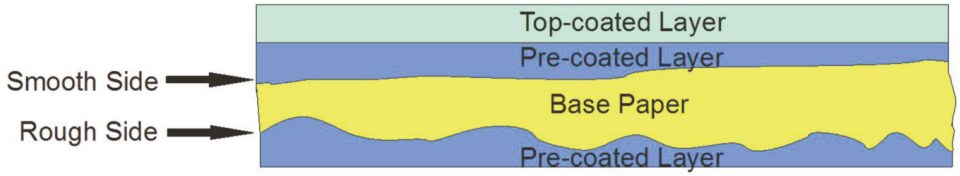

Figure 2 - *Schematic cross section of the final double coated paper samples.*

strip in a helicoidal form. Twelve samples are cut out of the 14 cm wide trip using a template 12.5 cm by 40 cm for a total area of 500 cm² per sample. In parallel, a sample with the same size (500 cm²) is cut out from the "uncoated paper" (it is actually the pilot precoated samples) portion from each CLC run. The "uncoated paper" sample serves as the reference to calculate precisely the coat weight applied with the CLC. The target coat weight is 12 ± 0.5 g/m². All 500 cm² top coated samples are weighed and only the samples within a ± 0.5 g/m² tolerance are kept for the study. A minimum of 15 CLC samples at the correct coat weight have been prepared for each precoat/topcoat combination.

All CLC top coated samples have been calendered with a laboratory supercalender containing 2 nips formed by 2 cotton rolls and one steel roll. The calendering is performed to obtain the 70 gloss target for the control condition (Group 0) for each latex used in the study: i.e. S/B/ACN latex, S/A latex, and S/A/ACN latex. Once the calendering conditions were found for each latex, all other group samples containing the same latex were done using the same latex calendering conditions. The laboratory calendering conditions are listed in Appendix (Table A6).

2.2 Mercury Intrusion

The mercury intrusion is performed with a Micromeritics Autopore III that allows a maximum pressure to be applied of 414 Mega Pascal (MPa) corresponding to about a 0.004 µm Laplace throat diameter (minimum pore dimension that can be measured). The equilibrium pressure time is set to 60 seconds. The mercury intrusion volume is obtained by measuring the variation inside a calibrated capillary tube (stem) that prolongs a bulb or sample holder.

All mercury intrusion data are normalised with a measure of the empty penetrometer, with no sample inside the penetrometer bulb (or blank), to allow for the penetrometer chamber deformation under pressure, mercury compression, and compressibility of the solid phase of the sample. The use of the blank penetrometer correction is explained below in the equation used for the Autopore to calculate the true volume intrusion in the sample. It is described in an article by Gane *et al* (1996). A typical mercury intrusion curve obtained from raw data is presented in Figure 3 which shows the volume intruded by mercury as a function of the pore size being intruded; such curve are typically called "pore distribution curves".

An important experimental procedure point to provide good test accuracy is the method used to set-up the paper sample to be analysed. The method is described by Ridgway and Gane (2007). The mercury intrusion test generates a data file with a series of results with pressure related to the volume of mercury intruded in the sample, from atmospheric pressure, about 0.1 mPa up to 414 mPa. The data file also contains the desorption data or decrease in volume when the pressure is released. The difference between the upward and downward curves is called hysteresis. As the file contains only raw untreated data, the data may and must be normalised to enable proper analysis of the porous structure under investigation.

Analysis of pore size distributions obtained by mercury intrusion

We have proposed a new method (Matte *et al*, 2009a, 2009b) to extract pore distribution using successive corrections from either a precoat or a top coat layer, calendered or not, from a correction of the data based on the analysis of the base uncoated or precoated or uncalendered paper and information from the analysis of

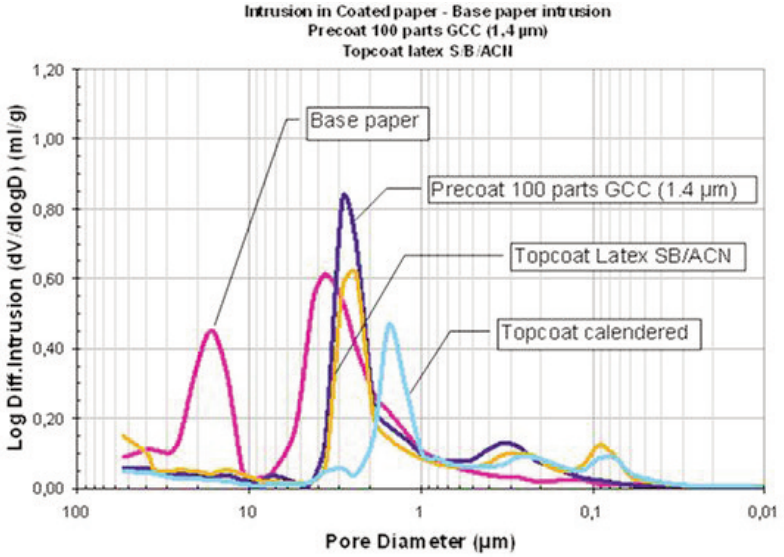

Figure 3 - *Pore distribution as a function of pore diameter (not normalised). The area of interest is as the left part of the graph, corresponding to pore diameters 0.8-0.9 µm and below.*

the hexadecane imbibition technique. In essence, in the normalization technique, and only for uncoated base stock papers, we used the hexadecane analysis to determine the cut-off points for low mercury intrusion pressures. In a paper sample, the very large pores, defects or mercury occlusions (Ridgway and Gane, 2007) generate a high absorption volume of mercury and affect the total pore volume results.

The interstices and defects that provide artificial information (artefacts) are thus removed from the basic data file to ensure a good reliability and accurate analysis of the test. Very simply, by mathematically removing the corresponding base paper pores, we obtain normalized values corresponding exclusively to the coating structure itself. Figure 4 illustrates the principle of normalization for removing the data corresponding to the base paper in the pore size of interest.

It should be noted that, although of apparently minor importance, the removal of pores related to the paper base stock modifies the distribution for the pores of double coated layer as can be seen from the decreases in the maximum pore volume (in mL/g). One hypothesis for doing so is that the interaction at the boundary between

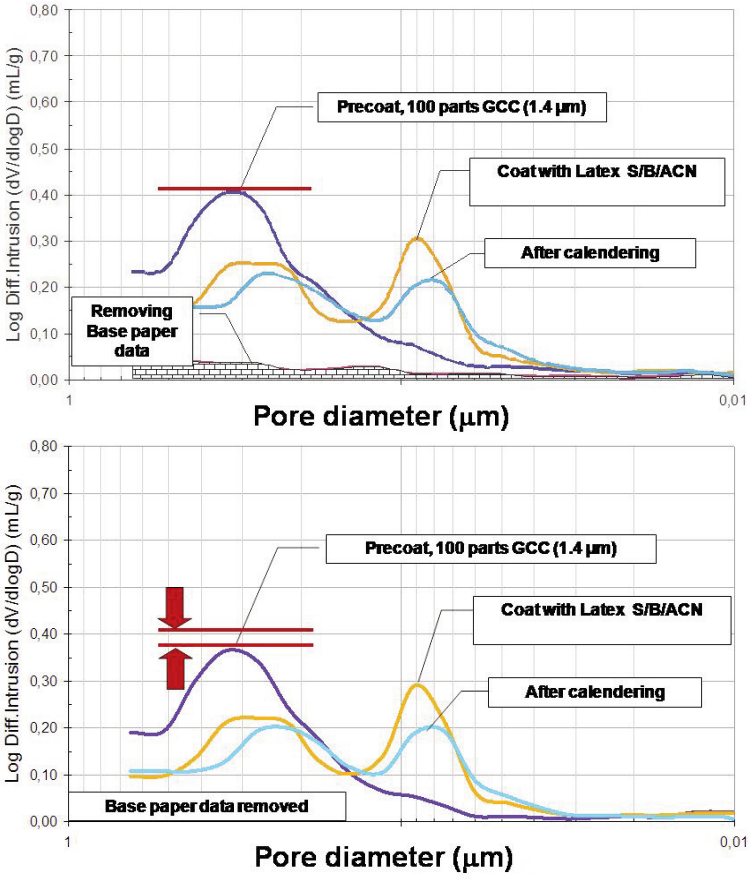

Figure 4 *– Schematic illustration of the procedure used for removing the pore data related to the paper base stock.*

paper base stock and the precoat layer is neglected: *i.e.* it is surmised (although physically wrong) that the layers can be completely separated. According to pure physics, the medium is continuous so no clear separation line can be identified (see Figure 1).

The same procedure has been applied to separate the distribution of the pores of topcoat layer from the precoat layer, as illustrated in Figure 5. Due to the fact that the procedure is basically of a mathematical nature (data from pores corresponding to the previous layer are deducted from the overall curve), the method may produce some artefacts that appear as negative values. It is however of little significance as a) only the "positive" pore are considered, b) the artefact is due to the natural pore variations occurring in the paper samples (the mercury intrusion test being destructive), and c) the procedure will create the same artefacts for all samples. Indeed, the repeatability of the procedure was found to be very good as, when samples with different topcoat (due to various latexes being used in the topcoat), the precoat distribution curves were almost identical.

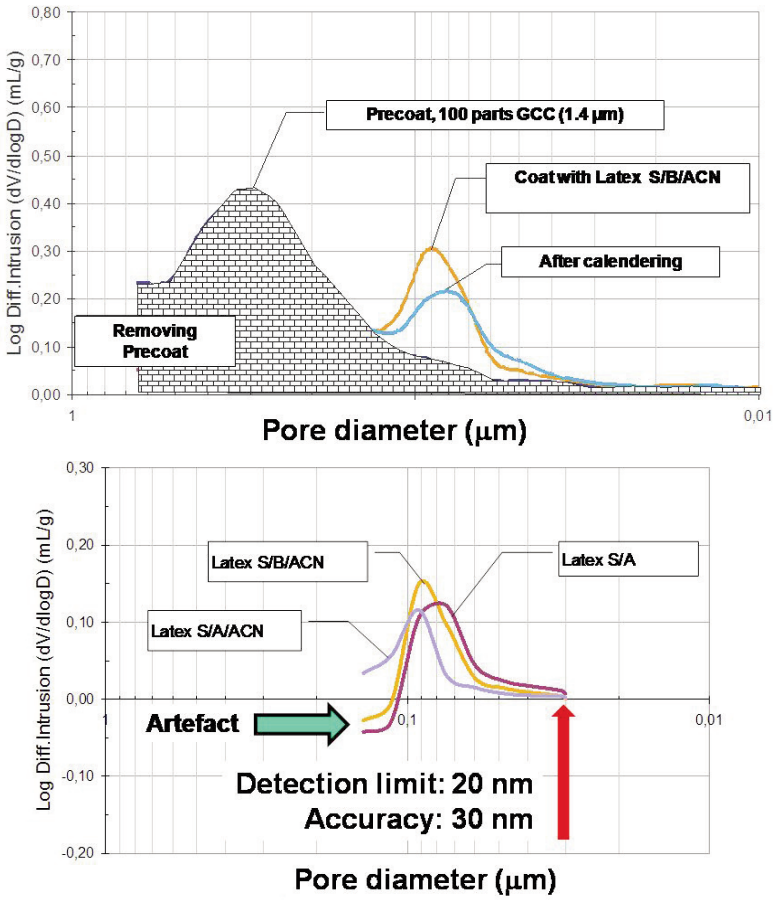

Figure 5 - *Schematic illustration of the procedure used for removing the pore data related to the precoat. After precoat data removal the negative values obtained for the topcoat above 0.1 µm are mathematical artefacts.*

2.3 Deltack

The Prüfbau Deltack method has been developed to simulate conditions occurring during commercial printing, mainly to appraise ink film splitting forces. It should be emphasized that the Prüfbau Deltack results are dependent on the printing speed, the printing temperature, the printing tension, the substrates, and of course mainly the substrate surface properties.

The instrument used in our study is a Multipurpose Ink Tack Measurement System Deltack from the company Prüfbau, Munich, Germany. The instrument settings are described in Table 2; the setting we used is "Web Offset". The paper strip used had a dimension of 5.4 cm width by 30 cm length. The ink used is a heat-set printing ink 40 8020 (Michael Huber, Munich, Germany). The ink set-up for the test is for "web offset"; *i.e.* 150 mm^3 of ink, 30 seconds for inking time on the inking unit, and 30 seconds for ink time on the printing form.

We followed the Deltack procedure by Omya (An. 2007) but with only 2 tests per side. The test conditions were: printing speed, 1 m/sec; printing force (unit A) 1000 N, printing force unit B, 810 N; delay between printing, 1 second; number of measurements, 30 per test; and ink volume 150 mm^3.

Instrument Setting	Web Offset
Measuring Mode	Mode X
Measuring Unit	1
Printing Tension	1000 N
Printing Tension for Splitting – Print Unit A	1000 N
Printing Form – Print Unit B	Metal 5 cm Width
Printing Form for Splitting	Rubber Green 5 cm width
Print Sample Carrier	Rubber
Speed for printing and Splitting	1.0 m/sec
Minimum Waiting Time after Printing	3 sec
Measuring Interval	1 sec
Number of Measuring Cycles	30
Mean Value Range	80-170 mm

Table 2 - *Prüfbau Instrument Settings for Sheet Offset and Web Offset*

Analysis of Deltack curves to obtain the maximum tack force

The ink setting on the calendered samples is evaluated with the Deltack method. An example of the curves obtained with the method is illustrated in Figure x. The method was developed for testing ink setting on coated paper grades. It measures

the tack force as a function of time which is determined by the interactions of the ink with the coating surface, the coating structure, and the ink on the tack disc.

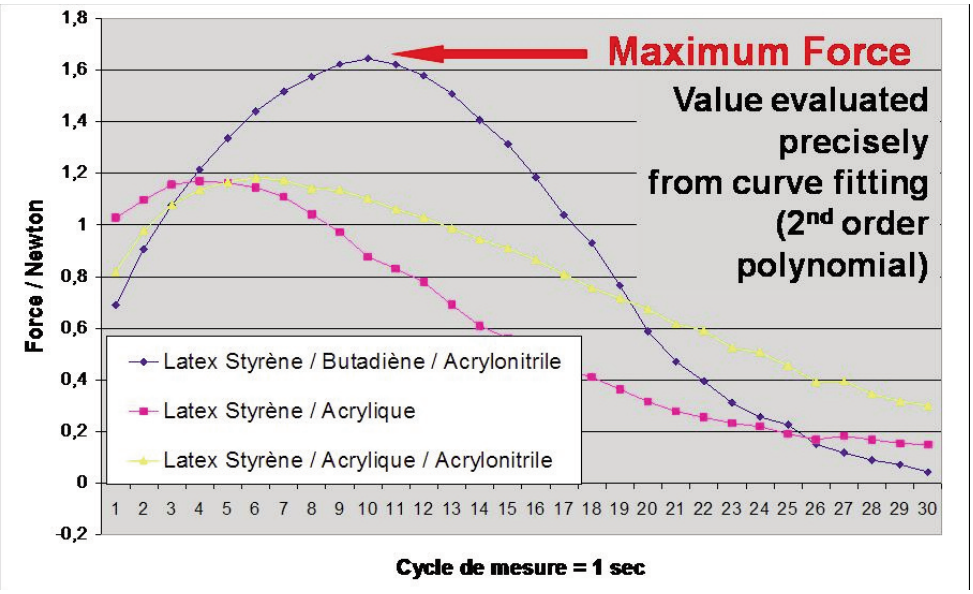

Figure 6 - *Example of tack development from a Deltack test curve.*

The standard laboratory Deltack printing curves presented in Figure 6 indicate that the tack force increases to a maximum then decreases. Both the maximum in ink tack force and the time it takes to reach the maximum (as evaluated by the measuring cycles) or "ink setting time" may be used to compare the curves. In our study, we propose to calculate the maximum ink tack and ink setting time for all curves using second degree polynomial as $y = ax^2 + bx + c$ with y the tack force value (in Newton) and x the time (in seconds).

It should be emphasized that the polynomial proposed is merely empirical in order to treat the data in a coherent, repeatable, and unbiased fashion as the complete curves found with the Deltack method do not necessarily all have an exact second degree polynomial shape. Indeed, to be able to use a second order polynomial, a part of the curve end have been, upon need, truncated to insure a good fit of the polynomial shape in the corresponding x-interval of the curve, *i.e.* near and around the maximum tack force value. As the determination coefficients (r^2) found were all above 0,99, the truncation results in a very good correlation between the Deltack curves and the polynomial fit, and therefore a very accurate determination of both the maximum tack force and the time to attain it.

An evaluation of the initial ink setting, driven by the solvent loss from the ink to the coating pores, is provided both by the tack build-up slope to the maximum tack, and by the time necessary to reach the maximum in the ink tack force. The tack decay is the start of the final drying process where enough solvent is lost from the

ink to provide the dry, non tacky, printed surface. The porosity, pore size, and total pore volume are known to have a great impact on ink setting (Lee, 1974, Okomori and Lepoutre, 1998, Kugge, 2004). Latex chemistry also affects the ink setting rate. The two considerations mean that ink setting is controlled by capillary absorption in the coating pores as well as ink absorption by the latex (Gane et al, 2000, Ström, 2005, Rousu *et al*, 2002). The Deltack approach is therefore a great tool to relate the printing characteristics of our samples to the structure modification brought about by modifications in the precoat and topcoat formulations.

3. Results and Discussion

3.1 Effects of 20 parts clay substitution in the precoat layer (Group 1)

The Group 1 includes 5 different conditions. The first condition has a precoat formulation that includes 100 parts GCC (1.4 μm) and is considered as the reference comparison point. The 4 other conditions are 80 parts GCC (1.4 μm) as in the reference but now with 20 parts clay having a different particle size distribution, and aspect ratio, as listed in Table 3. In essence, the 20% clay substitution is the variable between each formulation. The aspect ratio of the clay has not here been considered as a key variable (as it will be seen from our results).

Precoated formulation	Group	Formulation number
100 parts GCC (1.4 μm)	Control	3 topcoat = 3 samples
20 parts High glossing clay (0.469 μm) 20 parts No.2 clay (2.13 μm) 20 parts delaminated clay (5.312 μm) 20 parts High aspect ratio clay (6.329 μm)	Group 1 20 parts clay substitution	3 topcoat x 4 precoat = 12 conditions

Table 3 - *Conditions for the 20 Parts Clay Substitution - Group 1*

Figure 7 shows the total pore volume for the combined precoat/topcoat layers structure as a function of the clay average particle size in the 20 part substitution. The precoat only curve (without topcoat) is used as a reference for the initial structure before topcoat application. A curve was found after calendering of the topcoat. For both uncalendered and calendered samples, the total pore volume of the precoat/topcoat layers increases with the pigment size used as the 20 parts replacement in the precoat. Both for the uncalendered and the calendered samples, the latex S/A/ACN shows a higher pore volume than the other latexes (S/B/ACN and SA) notwithstanding the fact that the pressure we use to obtain a target gloss of 70 is about 20.7 bar for the S/A/ACN latex compared to 34.5 bar for the 2 other latexes. We may conclude that the difference in structure, already present in the uncalendered samples, is maintained in the calendered samples.

As far as gloss development is concerned, the acrylonitrile (ACN) is known to improve gloss development: it is probably the reason why the pressure needed to obtain a 70 gloss is lower for the S/A/ACN latex. However, it does not occur for the S/B/ACN latex. The gel content of the S/B/ACN latex being lower than the

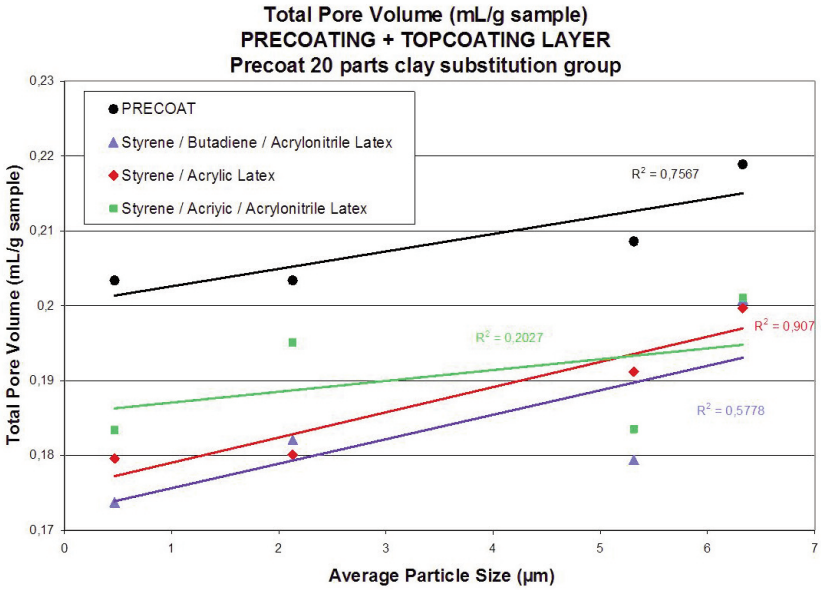

Figure 7 - *Total Pore Volume (TPV) Uncalendered Paper for Group 1 - Comparing the 3 latexes*

S/A/ACN latex might be the reason why the calendering pressures to obtain a 70 gloss are the same for the S/A and S/B/ACN latexes.

Figure 8 presents the average pore diameter of the precoat/topcoat layer structure to increase with the pigment size of the precoat 20 part substitution. It is apparent that the precoat structure is more open with larger particle size pigment than with smaller particle size pigment used in the 20 parts substitution. The effect is less apparent for the precoat/topcoat combined structure, whatever the latex used.

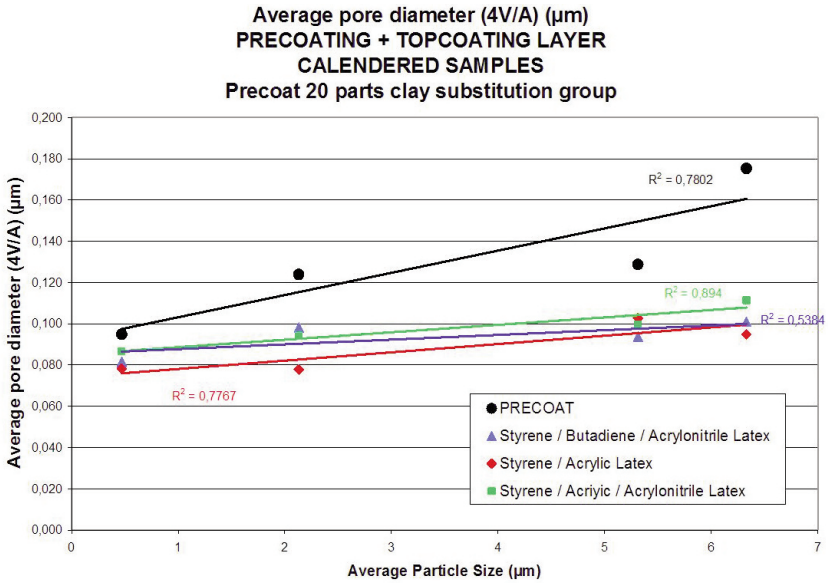

Figure 8 - *Average Pore Diameter (APD) Calendered Paper for Group 1 - Comparing the 3 latexes*

Therefore, we should look at the topcoat structure only to analyse the influence of the precoat 20 part pigment substitution.

As said previously, the increase in total pore volume as a function of the pigment particle size in the precoat layer needs further explanation. Due to the fact that both Figures show that the precoat total pore volume increases with the particle size, we may surmise that it is solely due to the increase in the precoat. However, as can be seen in Figure 9, the topcoat total pore volume increases with the pigment average particle size in the precoat. It is true for the 3 different latexes used in the topcoat although the topcoat layers have all the same pigment system (70 parts GCC and 30 parts N°1 glossing clay). It can then be concluded that the precoat structure has a direct effect on the structure of the topcoat. We propose that three physical principles may explain such an effect:

1. forced penetration of the topcoat coating colour in the precoat structure: an open structure with large pores (as defined by pore diameter) bringing about more penetration than a closed structure with small pores,

2. capillary penetration within the precoat structure: smaller pores favouring capillary penetration,

3. preferential topcoat pigment penetration within the precoat structure: smaller pigments (N°1 high glossing clay) penetrating more easily the precoat structure than larger size pigment (GCC).

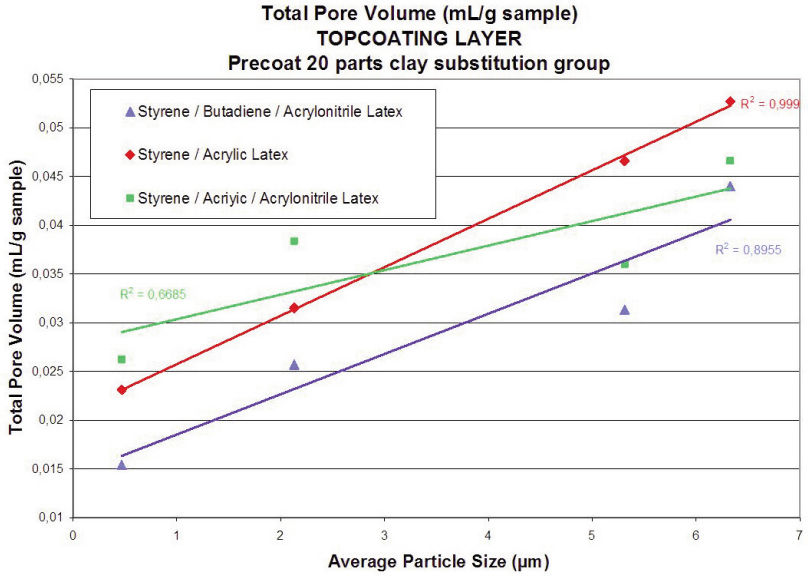

Figure 9 - *Total Pore Volume (TPV) Topcoated layer for Group 1 as a function of the particle size of the precoat layer – Comparison of the 3 latexes.*

Forced penetration implies that larger pores lead to more penetration of the topcoat layer within the precoat layer: i.e. leaving less coating layer on top and subsequently a smaller pore volume. According to the fact that the topcoat pore volume increases (linearly, as seen in Figure 9) with the precoat average particle size, this hypothesis can be ruled out: the forced penetration is not the right explanation.

The effect of capillary penetration can be further analysed by looking at the average pore diameter of the topcoat layer. For the topcoat structure with the S/A/ACN latex, Figure 10 shows that the pore size of the topcoat is independent of the pigment average particle size in the precoat. The increase in pore volume can then only be accounted for by a large number of pores of the same diameter. In other words, for a close structure in the precoat, there is less pores remaining than in the open structure. It means that more coating colour penetrates the precoat structure when pores are smaller: it can only be explained by capillary penetration being favoured by smaller capillaries, here smaller pore sizes (in the precoat structure). We conclude that capillary penetration should be considered as an acting force as illustrated in Figure 11 (a).

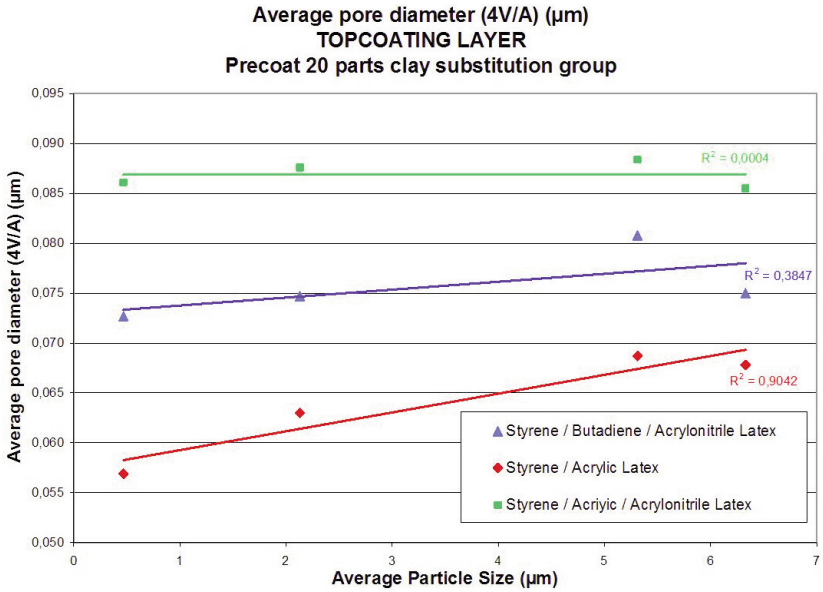

Figure 10 - *Average Pore Diameter (APD) Topcoated layer for Group 1 as a function of the particle size of the precoat layer – Comparison of the 3 latexes.*

However, when analyzing the topcoat structures related to the S/A and S/B/ACN latexes, we see that the average pore diameter increases slightly, but significantly, with the pigment average particle size in the precoat. It means that another phenomenon is also taking place. We propose "preferential topcoat pigment penetration" in the precoat as the solid phase of the topcoat coating colour contains two pigments of different sizes (around 0.15 - 0.20 µm for the clay and around 0.66 µm for the

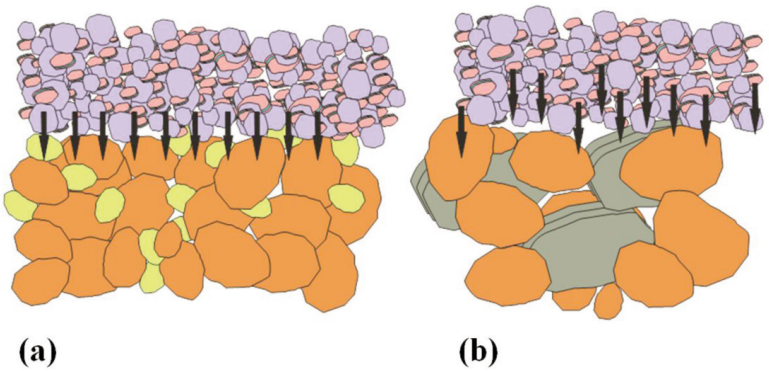

Figure 11 – *(a) Capillary theory related to smaller pores in the precoat. Topcoat: GCC is in purple-blue, clay in light red. Precoat: GCC is in orange and N°1 fine clay is in yellow. (b) Preferential movement theory related to bigger pores in the precoat. Topcoat: GCC is in purple-blue, clay in light red. Precoat: GCC is in orange and high aspect ratio clay is in grey.*

GCC) as illustrated in Figure 11 (b). Large pores in the precoat may absorb smaller pigments from the topcoat, whereas leaving a larger pore structure in the topcoat. For these two latexes, we surmise that there is a combination of the two phenomena: capillary penetration and preferential pigment penetration.

Another conclusion from present analysis is that the key information relating the structure of the topcoat/precoat layer will be deduced from the analysis of the maximum tack force (and not of the time needed to attain such maximum) as a function of both the pore volume, allowing for the capacity to absorb a given volume of ink, and the average pore diameter, to take into account the capillary phenomenon.

Figure 12 shows the maximum (tack) force as a function of the total pore volume (a) and the average pore diameter (b) of the topcoat/precoat structure. In addition to the grouping related to the 3 latexes (represented by 3 different lines), we find that an apex (minimum for the volume, maximum for the average pore size) occurs for the S/B/ACN and S/A latexes. The fact that no apex occurs with the S/A/ACN latex might simply be due to the lack of data at low values in either pore volume or diameter. Considering, for instance, the curves (in red) corresponding to the S/A latex, two different situations occur.

On the one hand, the same maximum tack force originates from structures having two largely different pore volumes (Figure 12a) but the same average pore diameter (Figure 12b), as seen from data points corresponding to the downward arrows. On the other hand, the same maximum tack force originates from structure having the same pore volume (Figure 12a) but two largely different average pore diameters (Figure 12b), as seen from data points corresponding to the upward arrows.

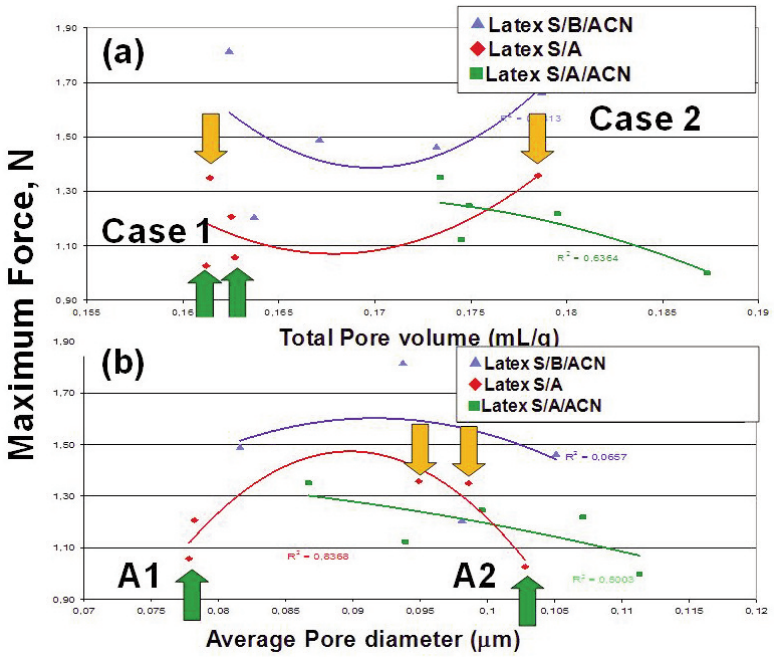

Figure 12 - *Maximum tack force (Deltack) versus total pore volume (a) and versus average pore diameter (b) for 20 parts clay substitution group.*

In other we have two opposite cases:

- Case 1: same maximum force obtained for structures presenting similar total pore volumes but very different average pore diameters, and

- Case 2: same maximum force obtained for structures presenting very different total pore volumes but similar average pore diameters.

Obviously to explain such behaviour of the topcoat/precoat structure, at least two phenomena must occur and have opposite effects. Let us consider the case where we obtain the same maximum tack force with the same total pore volume (upwards arrows – Figure 12a) and largely different pore diameters (upward arrows, Figure 12b). To understand the phenomenon that we surmise to be related to the topcoat/precoat structure as we have illustrated in Figure 11, we need to have some information on the topcoat structure only. Such information is provided by the Figures 9 and 10 which show both the average pore size and the pore volume of the topcoat to increase linearly with the pigment size of the precoat structure (20 parts substitution). In Figure 12a, the available volume for ink penetration provided by the topcoat/precoat structure is the same, and we could conclude that the ink transfer is the same and that the remaining ink layer on top of the topcoat structure is the same, providing the same maximum tack force.

However, we propose here that the maximum tack force is due to more complex phenomena as the average pore size of the two structures is widely different: *i.e.* the ink transfer should not be the same (De Grâce et al, 1984, 1987). In essence, we propose that ink transfer is different because the topcoat structures are different. In effect, the arrow (A1) corresponding to the low pore size (low average pore diameter) in the precoat/topcoat structure corresponds to very fine pores and a very small volume in the topcoat structure (see Figures 9 and 10). In parallel, the arrow (A2) corresponding to the high pore size (in precoat/topcoat structure) corresponds to larger pores and larger volume in the topcoat structure. Practically, it means that ink layer remaining of the surface in ''A1'' will be thicker than in ''A2'' (smaller pores and smaller available volume).

Considering the actual sizes of these pores, it also means that the structure with very small pores will favour, due to capillary penetration, the preferential absorption of ink solvent. In essence we will end up with a thicker ink film but with less solvent, *i.e.* a tackier ink. In the case of the larger pores, there will be no or less penetration of ink solvent. It is therefore quite feasible that the two effects being opposite, we will end up with the same maximum tack force. The phenomenon is illustrated in Figure 13.

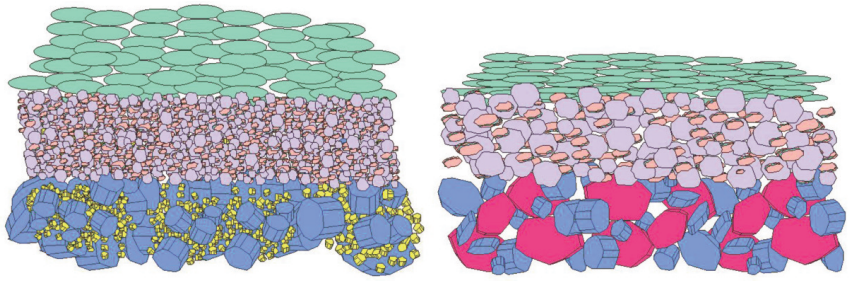

Figure 13 - *Ink film thickness related to an equal ink tack force and the precoat structure: close precoat structure (left) and open precoat structure (right)*

The explanation for obtaining the same maximum force with different ink film thicknesses, as seen in Figure 13, is coherent with variation in tack forces as follows:

- Case 1: is the case for a thicker ink film due to selective preferential filtration of ink solvents but although an ink with higher viscosity (than for case 2)

- Case 2: is the case for a thinner ink film resulting from a whole penetration of ink without (or with little) ink/solvents separation; i.e. no or little filtration occurring but then resulting in an ink with lower viscosity (than for case 1).

Going back to the Stefan's law (Mangin *et al*, 1990) describing the maximum tack force F as a function of the separation velocity Vs, the ink viscosity η, the area in contact with ink A, and the cube of the ink film thickness X as equation below:

$$F = \frac{V_s \eta A}{X^3}$$

Obtaining the same forces (F1 = F2) for different ink thicknesses (X1, X2) with various viscosity (η_1, η_2) implies that

$$F_1 = \frac{V_s \eta_1 A}{X_1^3} \quad \text{(equation 2)}$$

$$F_2 = \frac{V_s \eta_2 A}{X_2^3} \quad \text{(equation 3)}$$

Equations 2 and 2 result in $\frac{\eta_1}{\eta_2} = \left(\frac{X_2}{X_1}\right)^3$ equation 4.

Equation 4 is in agreement with proposed theory and mechanisms as the ration of the viscosity is inversely proportional to (the cube of) the ink film thicknesses.

Furthermore, we also know that some precoat formulations containing high glossing clay (0.469 μm) and No. 2 clay (2.13 μm) produce a larger amount of small sized pores in the final pore size distribution after topcoat application and calendering than the precoats containing delaminated clay (5.312 μm) and high aspect ratio clay (6.329 μm). It is also known that for coatings of equal pore density (number of pores per unit area) the ink sets faster due to the larger pores. Compared at equal pore volume which is a function of size and pore density, coatings with smaller pores set ink faster because of the larger number of sites available for ink penetration by capillarity (Preston *et al*, 2001).

When analyzing the situation (case 2) where a) the available pore volume of the topcoat/precoat structure is widely different (downwards arrows, Figure 12a) but b) the average pore diameter of the topcoat/precoat structure is the same (downwards arrows, Figure 12b), then, a similar analysis can be performed. In essence, we will end up with two different ink layers because the topcoat structure is modulated by the precoat structure. Therefore, due to the preferential solvent penetration, the maximum tack force will still approximately be the same. One should note that we have taken two extreme cases and that this compensation effect of solvent penetration controlling the ink tack and ink transfer controlling the ink thickness (and therefore also the tack force) is necessarily valid for all intermediary cases.

It should also be noted that the mechanism that we are here proposing is complementary to previous works and models proposed by the Gane group (Gane *et al*, 2000, Rousu et al, 2001, 2002). The slow ink setting trend containing latex with low Tg and acrylonitrile is seen for all the precoat and topcoat combinations. Latexes S/B/ACN have an ink setting behaviour that follow the coating porosity while latex S/A and S/A/ACN have a slower ink setting than could be predicted from the sole topcoat/precoat porosity.

The slow ink setting trends for topcoats with the latex containing acrylonitrile could be explained by the slowing effect of acrylonitrile and the well-known rule in coating formulation and physics: latex is about 10% of the coat weight, 20% of the coating volume, and 50% of the coating surface. Indeed, Rousu *et al* (2002) showed that low latex solubility parameter (butadiene < styrene = acrylate < acrylonitrile) leads to a large effect of oil interaction. Furthermore, latexes with low glass transition temperature (Tg) and percentage of gel (gel, %) show an increased interactivity with ink oils (Van Gilder and Purfeest, 1994). It also means that the setting of the ink can also be adjusted to be faster or slower according to the choice of ink. It implies that the differences we have analysed could be greater or smaller depending on the ink used in the printing operation.

Finally, we used a lower calendering pressure for the S/A/ACN latex coatings to achieve the same gloss target than all other coatings. The difference in calendering probably produces a slightly different connectivity for the coating pores compared to the other coatings. We have not further analysed such a probability.

Last but not least, the Deltack method is performed without fountain solution. The acceptance of different liquids (solvent, fountain solution, ink oils, etc.) to the pores will further complicate how the pore-to-throat diameter ratio, and the available volume of the small voids will influence the ink setting (and therefore the maximum tack force from the Deltack method). It is still unclear how the latex with the increased solvent absorption (lower solubility parameter) shows a faster ink setting, and the question remains if the latex swelling may partly close or not surface pores. Consequently, the latex swelling effect may further reduce the coating porosity and capillary absorption (Xiang *et al*, 2004, Hayes *et al*, 2000, 2003).

The last comment pertains to the solubility parameter of the solvent within the ink. As the difference between the solubility parameter of the solvent within the ink and the chemistry of the latex increases, the rate of solvent absorption decreases. The addition of acrylonitrile to a latex polymer decreases the solubility parameter compared to styrene butadiene latex. The result is that the difference between the solubility parameter of the solvent and the acrylonitrile latex that of the styrene butadiene latex, results in a decreased ink set rate for the acrylonitrile containing latex (Vyörykkä, 2007).

3.2 Effects of 100 parts clay substitution in the precoat layer (Group 4)

If the mechanism proposed here to explain the ink setting behaviour of Group 1 with a 20% replacement of clay by other pigments bringing about structural changes in the precoat/topcoat layer structures is valid, we should find the same pattern occurring when all pigments are replaced, as is the case for Group 4, with 100% substitution of the pigments in the precoat structure; *i.e.* when 100% of the precoat pigments are replaced by different pigments, in size, shape, and origin as presented in Table 4.

Similar to Figure 12, Figure 14 shows the maximum (tack) force as a function of the total pore volume (a) and the average pore diameter (b) of the topcoat/precoat structure for the 100% clay substitution (Group 4).

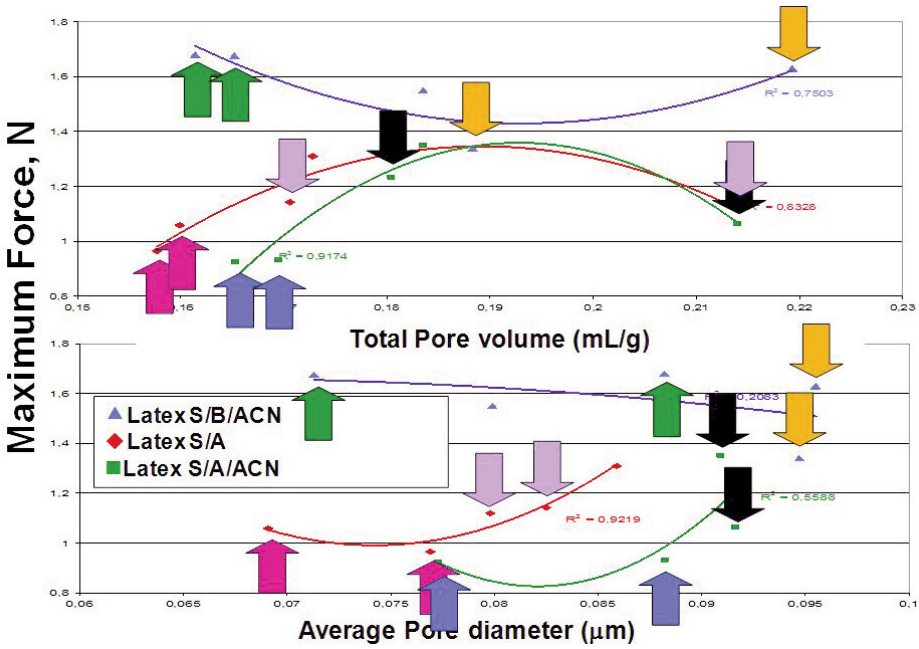

Figure 14 - *Maximum tack force (Deltack) versus total pore volume (a) and versus average pore diameter (b) for 100 parts clay substitution group.*

In Figure 14, the upward and downward arrows of the same colour indicate grouping corresponding to either case 1 (same maximum force obtained for structures presenting similar total pore volumes but very different average pore diameters) or care 2 (same maximum force obtained for structures presenting very different total pore volumes but similar average pore diameters). As expected from our proposed mechanism and theory, the maximum tack forces are the same for each individual grouping.

Precoated formulation	Group	Formulation number
100 parts GCC (1.4 µm)	Control	3 topcoat = 3 samples
100 parts BPSD GCC (0.659 µm) 100 parts BPSD GCC (0.3598 µm) 100 parts PCC (0.499 µm) 100 parts Brazilian clay (0.548 µm) 100 parts NPSD GCC (0.6593 µm)	Group 4 100 parts pigment substitution	3 topcoat x 5 precoat = 15 conditions

BPSD: broad particle size distribution NPSD: narrow particle size distribution.

Table 4 - *Conditions for the 100 Parts Clay Substitution - Group 4.*

The analysis of the structures of the samples obtained when substituting 100 part pigments for different pigments in the precoat layer structure allows us to confirm that the precoat structure greatly impact the final structure of coated paper. We have seen here the key importance of the particle size distribution and of the average particle size, and how they impact the precoat/topcoat structure. More specifically, we found, and explained how, the total pore volume is somehow inversely proportional to the particle size distribution. We also found that the total pore area decreases with particle size but, in the case of the broad particle size distribution pigment, it is inversely proportional to the particle size. Finally, as expected from pigment packing and influence on the coated layer pores, we confirmed that the average pore diameter is directly related to the particle size of pigments used in the precoat.

Last but not least, the mechanism we proposed to explain similar maximum ink tack force, as measured with the Deltack, with widely different pore structures, namely similar total pore volumes obtained with widely different average pore diameters, and largely different total pore volumes obtained with similar average pore diameters, has been validated and confirmed. As a reminder, the theory is based on the effect of preferential solvent penetration controlling the ink tack, and the effect of ink transfer controlling the ink thickness. We can then infer that such a finding somehow confirms and validates our proposed mechanisms and theory.

4. Conclusion

We have shown that the same ink tack could be obtained when printing in the exactly same conditions on very different pore structures, either with equal pore volume and very different average pore size, or on the contrary, with very different pore volume and the same average pore size. We have proposed a fundamental mechanistic approach to explain this particular phenomenon. The mechanism is related to the changes in topcoat structure originating from the different precoat structures. Overall, the structural changes in a complex two layer structure provided by the precoat/topcoat will modify how the ink and/or the ink solvent penetrate preferentially into a two layer structure thus resulting in a thick or thin ink layer with different final compositions which will provide the same tack force.

Another key conclusion related to 20 parts substitution in the precoat (Group 1) is that differences in printing properties as described by the Deltack analysis are mainly related to the type of latex used in the topcoat layer. The butadiene base latex always presents higher maximum tack force and time than the styrene acrylic. We surmised it was related to the gel content of the latex.

Considering that the most dramatic commercial change would be to “move to completely another type of pigment”, we looked how different pigment types

would modify the precoat structure and therefore the whole double-coated paper structure and properties. The analysis of the structures of the samples obtained when substituting 100 part pigments (Group 4) for different pigments in the precoat layer structure allowed to confirm that the precoat structure greatly impact the final structure of coated paper. We confirmed here the key importance of the particle size distribution and of the average particle size, and how they impact the precoat/topcoat structures.

Last but not least, the mechanism we proposed to explain similar maximum ink tack force, as measured with the Deltack, with widely different pore structures, namely similar total pore volumes obtained with widely different average pore diameters, and largely different total pore volumes obtained with similar average pore diameters, was fully validated and confirmed with the precoat layers containing very different pigment types.

Present work brings two important contributions to the understanding of the physics and structure of double coated paper, and more specifically on the effect of the precoat layer on the double coated paper structure and properties.

First, we have outlined a normalisation method to treat the mercury intrusion data in such a way that it is now feasible to extract the maximum amount of structural information on such data sets. The method allowed us to isolate the coating layers one from the other. It proposes a new way to treat mercury intrusion data sets to analyse the pore structure with good accuracy down to 30 nanometers, and probably lower. The method represents a new powerful tool to understand the flow dynamics at the nano level, for instance, as we have seen, how wet layers behave when applied one on top of the other. The new method enabled to segregate each layer structure separately, providing the potential to fine tune the analysis of multi-layered paper coating and to analyse how various coating colour formulations will affect each layered structure separately.

Second, we have developed a mechanism to explain how the same printing characteristics (as indicated by the maximum Deltack force) can be obtained with two completely different structures, namely structures with the same pore volume but very different average pore diameters, and structures with widely different pore volumes but (almost) identical average pore diameter.

From a commercial standpoint, we have demonstrated that the precoat has a more practical importance than usually accepted by industry practices. Generally, the precoat is more or less considered as a "layer filling-in surface defects and pores." We have shown here that the precoat is an integral part of the double coated paper structure and printing characteristics. In essence, it could be used to fine tune the desired double coated paper properties.

Literature Cited

Allem, R. and Uesaka, T.
1999 “Characterization of paper microstructure: A new tool for assessing the effects of base sheet structure on paper properties, Advanced Coating Fundamentals Symposium, Toronto, Canada: TAPPI Press.

Anonymous
Undated, Centre International de Couchage, www.coatercic.com, Pilot Coater Facility, Tool Coater, Production of Speciality papers, Trois-Rivières, Québec, Canada.

Anonymous
2007 “Lab Test Method - Deltack, Omya, Editor, Oftrigen, Switzerland. p.2.

De Grâce, J.H. and Mangin, P.J.
1984 “A mechanistic approach to ink transfer, Part I: Effect of substrate properties and press conditions”, Advanced in Printing Science and Technology, p.312.

De Grâce, J.H. and Mangin, P.J.
1987 “A mechanistic approach to ink transfer, Part II: The splitting behaviour of ink in printing nips”, Advanced in Printing Science and technology, p.146.

Drage, G., Vaugham, C., Henderson, K., Parsons, D.J., and Hiorns, A.G.
1999 “The influence of freesheet and groundwood basepaper formation on coated and printed paper”, TAPPI Coating Conference, Toronto, Canada: Tappi Press.

Eng, C.
2002 “Double layers coated paper picture”, Editor (and e-mail), Omya: Oftrigen, Switzeerland.

Gane, P.A.C., Kettle, J.P., Mathews, G.P., and Ridgway, C.J.
1996 “Void Space Structure of Compressible Polymers Sphere and Consolidated Calcium Carbonate Paper Coatings Formulation”, Industrial and Engineering Chemistry Research, 3(5): p.1753.

Gane, P.A.C., Schoelkopf, J., Spielmann, D., Mathews, G.P., and Ridgway, C.J.
2000 “Fluid Transport into Porous Coating Structures: Some Novel Findings. TAPPI Journal, 83(5): p.77-78.

Grön, J. and Rautiainen, P.J.
1999 “Coating solutions for wood-containing and woodfree paper grades,” TAPPI Coating Conference, Toronto, Canada: Tappi Press.

Hassell, M.V., Plasted, R.M., and Newberry, V.F.
1989 "Study of precoat pigments in double-coated paper and board", Pulp and paper Canada, 90(3): p.101-102.

Hayes, P.C., Bousfield, D.W., Kettle, J., Yang, X., and Hultgren, L.
2000 "Effect on Latex Selling on Ink Tack Build-up and Ink Gloss Dynamics", International Printing and Graphics Arts Conference: TAPPI Press.

2003 "Effect on latex swelling on ink setting on coated paper", Journal of Graphic Technology, 1(1): p.117.

Karathanasis, M., Carne, T., Dahlvik, P., Haugwitz, B., and Ström, G.
2001 "Importance of coating structure for sheet-fed offset print quality," Wochenbl Papierfabr., 129(7): p.426-432.

Kugge, C.
2004 "An AFM study of local film formation of latex in paper coatings," Journal of Pulp and Paper Science, 30(4): p.105-111.

Lee, D.I.
1974 "A fundamental study on coating gloss", Dow Chemical Corporation: Midland, USA.

Mangin, P.J., Silvy, J., and De Grâce, J.H.
1990 "Offset Linting Studies: Part II. Further Contribution to Linting Theories", 6th IPGAC, Vancouver, BC, Can., Preprints 109-119.

Matte, D., Mangin, P.J., and Daneault, C.
2009a "Precoat and topcoat effect on the final printability - Part 1: Coating structure analysis with mercury intrusion", 95th PAPTAC Annual Mtg., Proc.385-391, Montréal, Qc., Can.

Matte, D., Dimmick, A., Saari, J., Mangin, P.J., and Daneault, C.
2009b "Precoat and topcoat effects on final printability - Part 2: Coating structure analysis with mercury intrusion", TAPPI PaperCon 09, Saint Louis, Missouri, USA.

Okomori, K. and Lepoutre, P.
1998 "Effect of pigment size and shape distribution on the cohesion of pigmented coatings", TAPPI Coating / Papermakers conference, New Orleans, Louisiana, USA: TAPPI Press.

Preston, J.S., Elton, N.J., Legris, A., and Nutbeen, C.
2001 "The role of pore density in the settings of offset printing ink on coated paper", Advanced Coating Fundamentals Symposium, San Diego, California: TAPPI press.

Renvall, S.V., Rautiainen, P.J., and Rossitto, J.C.
1990 “Optimizing the Coating Process for Double-Coated, Wood-Containing Papers”, TAPPI Journal, 73(5): p.143-149

Ridgway, C.J. and Gane, P.A.C.
2007 “Bulk density measurement and coating porosity calculation for coated paper samples”, Coating and Graphic Arts Conference, Miami, FL, USA: TAPPI Press.

Rousu, S., Gane, P.A.C., and Eklund, D.
2001 “Influence of coating pigment chemistry and morphology on the chromatographic separation of offset ink constituent”, 12th Fundamental Research Symposium, Oxford, U.K.

Rousu, S., Lindström, M., Gane, P.A.C., Pfau, A., Schädler, V., and Eklund, D.
2002 “Influence of latex - Oil Interactions on Offset Ink Setting and Component Distribution on Coated Paper”, 2002 International Printing and Graphic Arts Conference, Bordeaux, France.

Ström, G.
2005 “Interaction between offset ink and coated paper - a review of the present understanding”, 13th Fundamental Research Symposium, Cambridge, UK.

Toivakka, M. and Nyfors, K.
2000 “Pore space characterization of coating layers. 2000 TAPPI Coating Conference and Trade Fair, Washington, DC: TAPPI press.

Van Gilder, R.L. and Purfeest, R.D.
1994 “Commercial six-colour press runnability and the rate of ink build as related to the latex polymer solubility parameter”, TAPPI Journal, 77(5): p. 230.

Vyörykkä, J.
2007 “Latex -Chemistry and Use in Paper Coating”, Pigment Coating Chemistry Course, Åbo Akademi University, Helsinki, Finland.

Xiang, Y., Bousfield, D.W., Hayes, P.C., and Kettle, J.
2004 “A Model to Predict Ink Setting Rates Base in Pore Size Distribution,” Journal of Pulp and Paper Science, 30(5): p. 13.

Zou, X., Vidal, D., and Allem, R.
2002 “Film Press for pigments coating: Coated paper quality and basestock effects,” TAPPI Metering Size Press Forum IV, Orlando, Florida: TAPPI Press.

Appendix

Latex	Tg temperature (°C)	Carboxyl°	Gel Content	Particle size (Å)
SBR latex	+17	Low	Low	1800
Styrene / Butadiene / Acrylonitrile	+10	medium	Medium	1400
Styrene/Acrylic*	+23	medium	High	1400
Styrene/Acrylic*Acrylonitrile	+40	medium	high	1400

Table A1- *Latex Characteristics used in the Study*

*Acrylic latex use the n-buthyl acrylate like second monomer

	Cond. 1	Cond. 2	Cond. 3	Cond. 4	Cond. 5
GCC (1.4µm)	100	80	80	80	80
High glossing clay (0.469µm)		20			
No. 2 clay (2.13µm)			20		
Delaminated clay (5.312µm)				20	
High Aspect Ratio clay (6.329µm)					20
Latex SBR	10	10	10	10	10
Optical Brightener Hexasulphonated	0.5	0.5	0.5	0.5	0.5
Calcium Stearate	0.4	0.4	0.4	0.4	0.4
Carboxy Methyl Cellulose(CMC)	0.7	0.7	0.7	0.7	0.7
Solids	66%	66%	66%	66%	66%

Table A2 - *Precoated Standard Formulations and 20 Parts Substitution*

Materials	*Cond. 17	Cond. 18	Cond. 19	Cond. 20	Cond. 21
BPSD GCC (0.659µm)	100				
BPSD GCC (0.3598µm)		100			
PCC (0.499µm)			100		
Brazilian clay (0.548µm)				100	
NPSD GCC (0.6593µm)					100
Latex SBR	10	10	10	10	10
Optical Brightener	0.5	0.5	0.5	0.5	0.5
Calcium Stearate	0.4	0.4	0.4	0.4	0.4
Carboxy Methyl Cellulose(CMC)	0.7	0.7	0.7	0.7	0.7
Solids	66%	66%	64%	64%	64%

Table A3 - *Precoat Formulations – 100 Parts Substitution*

* conditions 6-16 corresponding to Groups 2 and 3 are not presented here.

Coating Unit	Jet Applicator
Speed	1400 m/min
First Side to Coat	Rough
Coat Weight Application	12 g/m²
Moisture	4.5% for the rough side - 5% for the smooth side
Blade	0.457 / 84 mm / 45°
Dwell Length	350 mm
Jet Opening	0.9 mm
Jet Angle	34°
Gap – Jet/Baking Roll	10 mm
Beam Angle	45° - Constant Tip angle

Table A4 - *Precoat Operation Parameters – Coater*

Materials	Solids	Topcoat 1	Topcoat 2	Topcoat 3
BPSD GCC (0.659 µm)	76%	70	70	70
High glossing clay (0.469µm)	70%	30	30	30
Polyacrylate salt dispersant	40%	0.15	0.15	0.15
S/B/ACN	50	12		
SA	50		12	
S/A/ACN	50			12
Optical Brightener Hexasulphonated	100	0.7	0.7	0.7
Calcium Stearate	50	0.7	0.7	0.7
Ammonium zirconium carbonate	32	0.3	0.3	0.3
Carboxy Methyl Cellulose(CMC)	90	0.5	0.5	0.5
Solids		65%	65%	65%

Table A5 - *Topcoat Formulations used with the CLC*

Speed	14.7 m/min
Sample side on steel	Smooth
Number of passes	1
Steel Temperature	60°C
Nips Pressure - S/B/ACN latex	34.46 bar
Nips Pressure - SA latex	34.46 bar
Nips Pressure - S/A/ACN latex	20.68 bar

Table A6 - *Laboratory Calendering Conditions*